

Phase Retrieval to Monitor HST Focus: II. Results Post-Servicing Mission 4

Sami-Matias Niemi[†] & Matthew Lallo
Space Telescope Science Institute
December 7, 2010

ABSTRACT

Hubble Space Telescope (HST) focus has been monitored throughout the Observatory's life primarily using high-resolution imaging cameras. The preferred method to determine the focus position is a Phase Retrieval technique. It solves for certain Zernike polynomials such as focus, coma and astigmatism, by fitting a model Point Spread Function interactively adjusting the aberration parameters to observed data. In this report, we discuss results of the monthly focus monitoring program since the latest mirror move in July 2009. Since the primary purpose for this monitoring is to support accurate focus maintenance, we present a picture of the current focus state of the HST. We discuss focus measurements done with both the Advanced Camera for Surveys (ACS) and Wide Field Camera 3 (WFC3) and draw conclusions about their confocality. We also predict when the Observatory is going to be in the best focus. The spread in these predictions is large and arises from uncertainties, such as orbital thermal variations (breathing) and long-term trends, which are difficult to model. Our best estimate, based on the long-term historical focus trend, implies that ACS (and all science instruments confocal to it) is close to the best focus at the time of writing. There is tentative evidence that the best focus of WFC3 UVIS is $\sim 0.5 \pm 0.2 \mu\text{m}$ below that of ACS.

1 Introduction

The focus monitoring of the Hubble Space Telescope (HST) has always been performed with cameras capable of high-resolution imaging. Earlier in the mission the focus monitoring was

[†]niemi@stsci.edu

performed using Wide Field Planetary Camera 2 (WFPC2), while after the installation of the Advanced Camera for Surveys (ACS) its high-resolution channel was often favored. During the Servicing Mission 4 (SM4) of the HST in May 2009 a new camera capable of high-resolution imaging was installed on board the HST. Wide Field Camera 3 (WFC3) is a wide field imager, whose wavelength coverage ranges from the ultra-violet to the near-infrared. A reasonably fine pixel scale of the UVIS channel (at 500 nm the full width at half maximum is ~ 1.675 pixels) together with a high sensitivity and a large selection of filters makes it well-suited for a Phase Retrieval technique and for focus monitoring. The implementation of the WFC3 UVIS channel in our focus monitoring software is described in Niemi et al. (2010).

The monthly monitoring of the HST focus is important because the long term trend has shown that the telescope is shrinking (Lallo et al. 2005), thus, the secondary mirror has to be moved back to compensate. The secondary mirror has been moved approximately 25 times since launch, and the latest mirror move took place in late Servicing Mission Orbital Verification (SMOV) at 09:35 UTC, June 20th, 2009. This report describes the focus monitoring results since the mirror move, while the estimates and rationale for the SMOV adjustment are discussed in Lallo et al. (2010).

2 Measuring Focus

In 1997 John Krist and Christopher Burrows wrote a parametric Phase Retrieval software package called FITPSF that is suitable for HST focus monitoring (Krist and Burrows 1997). The software and its application to HST data is described in Krist and Burrows (1995), while the WFC3 UVIS channel implementation is discussed in Niemi et al. (2010). We refer the interested reader to these documents and will not repeat the discussion. Instead, we briefly describe the theoretical background of the Phase Retrieval technique.

2.1 Phase Retrieval

Phase Retrieval is a technique which is being used for the focus monitoring of the HST, and it concerns finding a solution to the phase problem. Briefly, Phase Retrieval consists of finding the phase that for a measured amplitude satisfies a given set of constraints.

A point spread function (PSF) for an optical system is determined by the amplitude and phase of the (approximately) spherical wavefront as it converges on the point of focus. The amplitude $A(u, v)$ measures the intensity of the wavefront at each point (u, v) on the sphere and is usually approximately uniform across the entire pupil, except where it is obscured by objects in the light path such as the secondary mirror and its support structures such as spiders and mirror pads. The phase $\Phi(u, v)$ measures the deviation of the wavefront from a sphere; a perfectly focused wavefront has zero phase error. If we assume that the wavefront is not strongly curved over the pupil, then the PSF $P(x, y)$ can be written as

$$P(x, y) = \left| \int \int A(u, v) e^{i2\pi(ux+vy+\Phi(u,v))} du dv \right|^2 . \quad (1)$$

Hence, a PSF is the square of the amplitude of the Fourier transform of the complex pupil function.

For the focus monitoring purposes, Phase Retrieval can be considered as the process of trying to recover the wavefront error $\Phi(u, v)$ given a measurement of the PSF. In practice, finding the focus consists of fitting a model PSF to data by varying the model parameters after utilizing a non-parametric calibration in the form of a “mirror map” (an image describing HST’s high and mid-frequency errors). Ultimately we require a mathematical connection between the model parameters and the optical aberrations to recover the focus.

2.2 Zernike Polynomials

The Zernike polynomials are a set of orthogonal polynomials that arise in the expansion of a wavefront function for optical systems with circular pupils (e.g. Wang and Silva 1980; Hu et al. 1989; Molodij and Rousset 1997). Hence, they can be used to describe aberrations within a circular aperture of an optical system and are also normalizable over an annular pupil, as with HST. Furthermore, they are related to the classical aberrations and thus provide a convenient mathematical expression of the aberration content in a wave front. Zernike polynomials have been used to examine, e.g., distortions in the HST mirror surface (Fienup et al. 1993; Krist and Burrows 1995).

The Zernike polynomials can be divided into odd and even polynomials and are invariant in form with respect to rotations of axes about the center of the pupil. They can be conveniently written in polar coordinates as products of angular functions and radial polynomials. Thus, the polynomials $Z_j(\mathbf{x})$ normalized on the telescope aperture are defined in polar coordinates (ρ, θ) by

$$Z_j^m(\rho, \theta) = \sqrt{n+1} \times \begin{cases} R_n^m(\rho)\sqrt{2} \cos(m\theta) & \text{if } j \text{ is odd} \wedge m \neq 0 \\ R_n^m(\rho)\sqrt{2} \sin(m\theta) & \text{if } j \text{ is even} \wedge m \neq 0 \\ R_n^0(\rho) & m = 0 \end{cases}, \quad (2)$$

where

$$R_n^m(\rho) = \sum_{s=0}^{\frac{n-m}{2}} \frac{(-1)^s (n-s)!}{s! \left(\frac{n+m}{2} - s\right)! \left(\frac{n-m}{2} - s\right)!} \rho^{n-2s}. \quad (3)$$

Now n is the radial degree of the j th polynomial and m is its azimuthal frequency. The visualization of Zernike polynomials, which can aid in understanding their nature, is shown in Figure 1, while the low-order Zernike polynomials are defined in Table 1. For the HST the most strongly varying aberration is the focus, described here by Zernike polynomial Z_2^0 (but sometimes referred to also within the HST mission as Z_4 under an alternative polynomial indexing scheme).

Table 1. Low-order Zernike polynomials.

Zernike Term	Aberration
Z_0^0	Piston
Z_1^{-1}	Y-tilt
Z_1^1	X-tilt
Z_2^{-2}	Y-Astigmatism
Z_2^2	X-Astigmatism
Z_2^0	Focus
Z_3^{-1}	Y-coma
Z_3^1	X-coma
Z_4^0	Spherical
Z_3^{-3}	Y-clover
Z_3^3	X-clover
Z_4^{-2}	Y-spherical astigmatism
Z_4^2	X-spherical astigmatism
Z_4^{-4}	Y-ashtray
Z_4^4	X-ashtray

3 Focus Monitoring Data

The ‘‘HST Cycle 17 and post-SM4 Optical Monitor’’ program (11877, P.I. Lallo) executes approximately monthly taking data with WFC3 UVIS channel as a primary instrument. This program was allocated, in total, 36 orbits for Cycle 17. Each visit of the focus monitoring program uses the WFC3 UVIS channel as a primary instrument, while the ACS WFC is used in parallel. Due to the overheads related to reading out the detector and memory dumps, the number of frames per orbit are rather limited, especially if full frame exposures with short exposure times are taken. We therefore modified the program during the Cycle 17 to optimize the collected data.

Visits 2 – 11 took two full frame exposures using WFC3 UVIS channel, which was centered on NGC-188-73, while ACS WFC took five full frame exposures in parallel. The full frame exposures are useful as they allow a field dependent PSF characterization and to characterize the focus changes as a function of detector position. The exposure times of these exposures were 15 and 30 seconds for WFC3 and ACS, respectively. Short exposure times are required to minimize the effect of ‘‘breathing’’ that causes the focus to change on short (a few minutes) timescales (see Lallo et al. 2005). The focus changes due to breathing can be modeled using a focus model (see e.g. Di Nino et al. 2008). However, the model correction is not perfect and it is therefore useful to try to optimize the data using a strategy to account for breathing.

To better cancel out the effect of breathing, we modified the program in February 2010 to take in total eight WFC3 UVIS 1 and 2 subarray exposures. We also increased the exposure time of WFC3 exposures to 30 seconds to get more well-exposed stars in the 2k by 2k subarray field. The first modified visit executed in April. Visits 12, 37, 38, 39, 40, in total

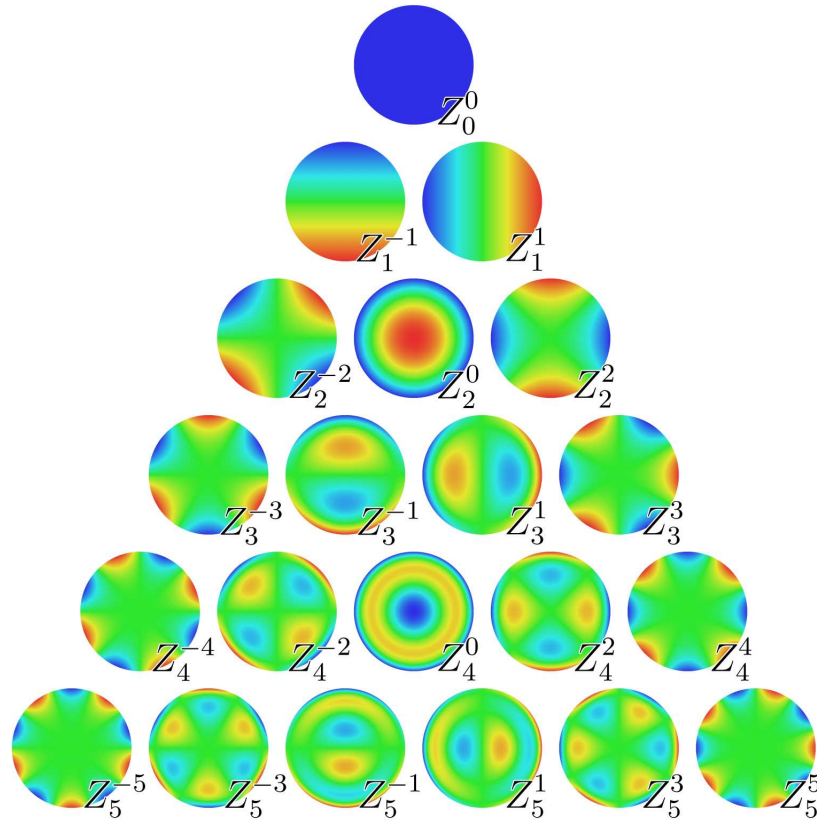


Figure 1. Selected Zernike polynomials in the unit disk. For definitions, see Table 1. Courtesy of Wikipedia.

five visits, used this modified scheme, while visits after August 2010 again use the original two full frame WFC3 exposure scheme.

In the modified program we set the UVIS-1 exposure to execute at the same time as the ACS WFC full frame exposure. Hence providing data that are well-suited to estimate the focus difference between the two cameras as breathing cancels out when simultaneously measuring the relative focus difference. In these simultaneous exposures the only effects contributing are the real focus difference including any variations or instabilities within the cameras and the intrinsic accuracy of the Phase Retrieval technique.

4 Results

Below we describe results derived from the focus monitoring data taken between August 2009 and September 2010. All datasets used in the analysis are listed in Table 4. Note that all defocus values referred to are in μm physical secondary mirror piston (axial motion), so that 1 μm defocus corresponds to 6 nm root mean square (RMS) wavefront error (WFE).

Figure 2 shows results and focus measurements of two single orbit visits that executed over eight months apart. The left-hand side plot shows focus measurements based on the first

visit that executed after the mirror move in July 2009. All the values in this plot have been corrected with the breathing model values. Without measurement errors and assuming that the breathing model would perfectly describe the focus changes, all points in the left plot would fall on a straight horizontal line. However, there is a fair amount of scatter between each measurement due to the imperfect Phase Retrieval and breathing model corrections. The large scatter for a given time shows the intrinsic inaccuracy of the phase retrieval when applied to moderately sampled PSFs. Even so, the average focus of the WFC3 UVIS channel agrees with the average focus of the ACS WFC channel within the standard errors of the mean. However, the WFC3 focus values tend to be closer to zero than ACS measurements. We will return to this in Section 4.3.

The right-hand side plot of Figure 2 shows focus measurements after the focus monitoring program was modified to use subarrays for WFC3. The defocus values in Figure 2 have not been corrected with breathing model values, and they clearly show a slope, which is consistent with the breathing. Again, however, the plot shows a large scatter between the measurements. Note that WFC3 focus values show a significantly smaller scatter than ACS results. This is likely due to the poorer sampling of a PSF in ACS, but can also be, at least partially, due to the relatively large charge transfer inefficiency (CTI) in ACS. The CTI will make the PSF more asymmetric than would optically be induced, affecting the fit of Zernike terms. With a perfectly sampled PSF, the CTI would not change symmetric Zernike terms such as focus, however, because of the less than optimal sampling in ACS WFC it is possibly that abnormal excess of counts in the PSF wing on one side may change the best fit of the focus term. This shows the in-built weakness of the Phase Retrieval technique: for moderately sampled PSFs it is not possible to completely separate the optical effects from, e.g., effects caused by imperfect electronics in a CCD.

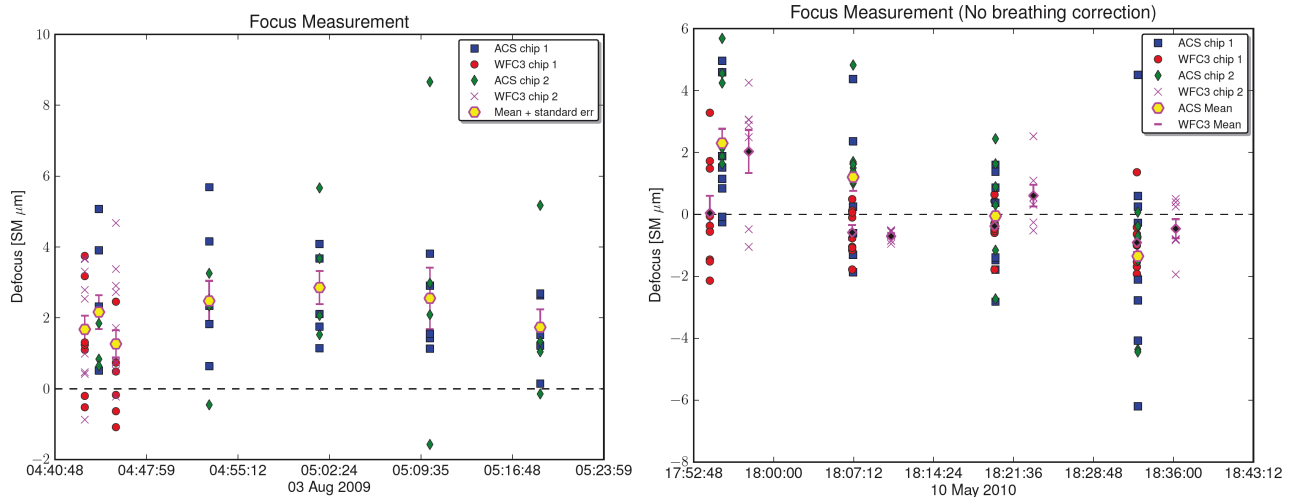


Figure 2. Focus measurements within a single HST orbit from visit 02 (left-hand side, executed on August 3, 2009) and 37 (right-hand side, executed on May 10, 2010) data of the HST focus monitoring program. Visit 02 measurements have been corrected with the breathing model values, while visit 37 are raw focus measurements without a model correction.

4.1 Historical Focus Trend

The HST focus monitoring has been performed since the launch of the Observatory. Hence, the historical focus trend goes back 20 years to April 1990. This historical trend is presented in Figure 3. The overall historical focus trend describes the shrinkage of the HST, i.e. how much the secondary mirror would have moved towards the primary if it had not been periodically adjusted. In 20 years the telescope has shrunk $\sim 150 \mu\text{m}$, which has been compensated by moving the secondary mirror (see also Lallo et al. 2005). This behavior is assumed to be due to moisture in HSTs graphite epoxy metering truss (Carter 1985) being forced out (“desorbed”) by space vacuum.

A double exponent of form

$$y = A_1 + A_2 e^{\frac{-x}{A_3}} + A_4 e^{\frac{-x}{A_5}} \quad (4)$$

has been found to well describe the historical focus trend of the HST. The latest fit, done in July 2010, gives the following parameter values:

$$A_1 \sim -4.27, A_2 \sim 57.19, A_3 \sim 410.17, A_4 \sim 103.29, A_5 \sim 2356.20$$

The double exponent and its best fit parameter values show that the shrinkage is slowing down. Thus, the need to back up the secondary mirror becomes less and less frequent over time.

Based on the focus measurements presented in this report and ongoing discussions of focus maintenance limits, the next mirror move may not take place before 2012. However, the monitoring will continue to assess the need of refocusing in the future. Although each instrument onboard the HST now has their own internal focusing mechanisms, it is generally assumed that it is more convenient to move the secondary mirror rather than try to refocus each instrument separately.

4.2 Focus Trend Since December 2002

Figure 4 shows the HST focus trend since the mirror move of December 2002. The left-hand side plot shows raw focus measurement values, while the right-hand side plot displays breathing model corrected focus measurements. Note the smaller scatter on the breathing corrected values, especially after the July 2009 mirror move (vertical dotted line at $x \sim 7020$). The mirror move of July 2009 is clearly visible in both plots, showing a break at $x \sim 7020$. The focus measurements obtained after the mirror move demonstrate: a) the success of the mirror move, and b) that the measured focus continues to follow the exponent fit done using the data since December 2002, but prior July 2009. The breathing corrected focus measurements between WFC3 UVIS channel and ACS WFC are in general within the measurement errors.

Figure 5 shows the focus trend since the mirror move of December 2002, but now the mirror move of July 2009 has been added to the older measurements. The figure demonstrates that the exponential shrinkage continues. The linear fit (green line) does not fit as

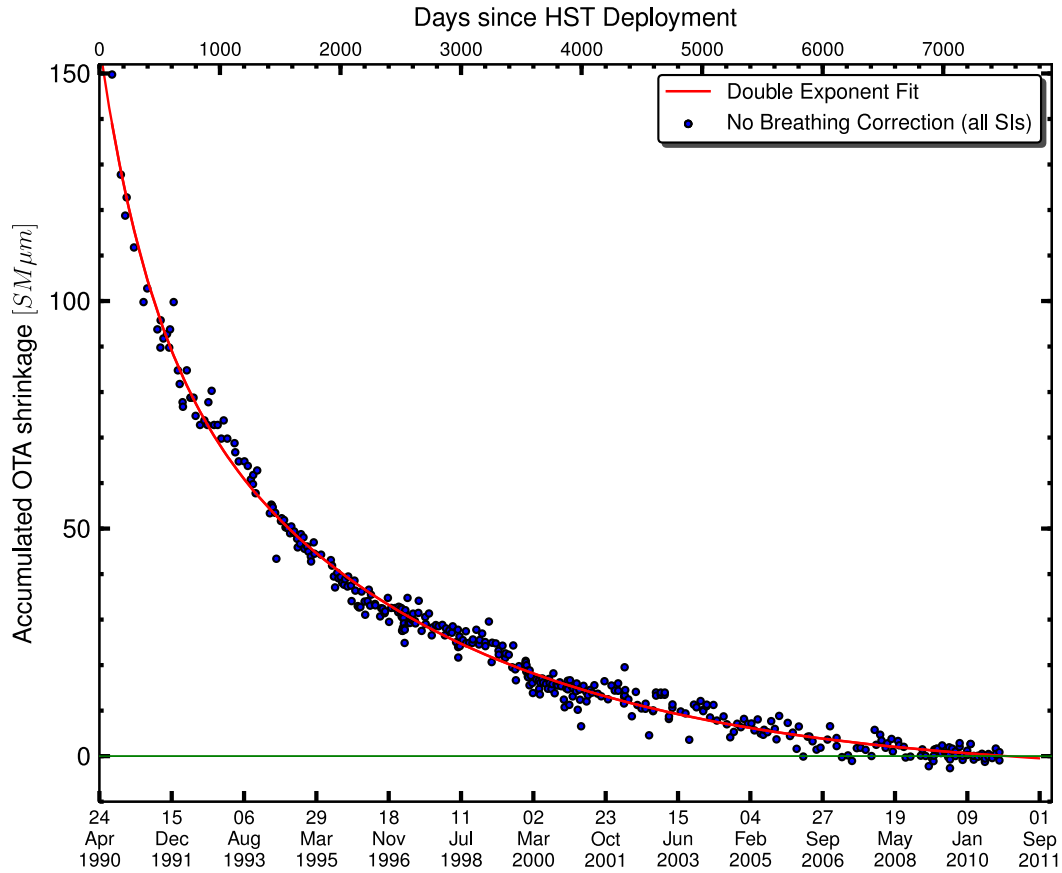


Figure 3. The historical focus trend since the launch of HST. The double exponent fits the measured focus values (all SIs) well. All values presented are direct measurements and have not been corrected for the breathing. The green horizontal line marks the zero-focus crossing.

well as the exponent. Note also the relatively small scatter between WFC3 measurements, in comparison to the old measurements. However, in general, WFC3 UVIS and ACS WFC measurements agree well, except in a few cases. The results of Figures 4 and 5 demonstrate the maturity of the Phase Retrieval when applied to WFC3 UVIS channel data.

Figure 5 also displays that breathing corrected WFC3 UVIS channel measurements tend to be systematically closer to the optimal focus than the focus measurements obtained using ACS WFC data. This implies that there is a small relative offset in the internal focus of WFC3 UVIS channel in comparison to ACS WFC.

4.3 Confocality of WFC3 UVIS and ACS WFC

Figure 6 shows the difference between the ACS WFC and WFC3 UVIS channel focus measurements for each visit. The relatively large scatter ($\sigma \sim 0.8$) between visits makes it difficult to draw any strong conclusions at this point. However, the figure clearly implies that

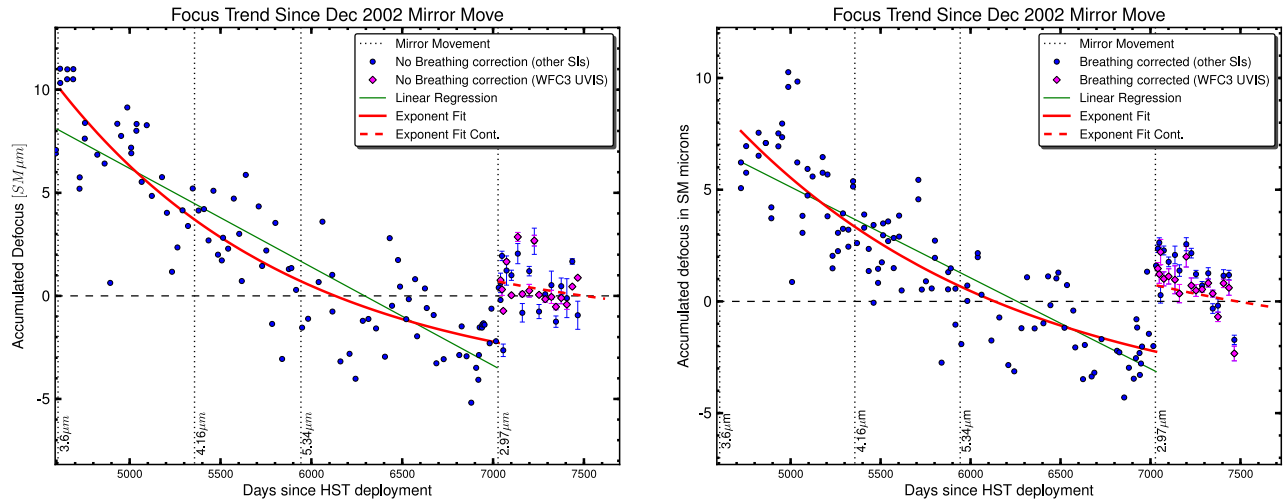


Figure 4. The two plots show all focus measurements since the mirror move of December 2002. Raw focus measurements are presented on the left-hand side, while in the right-hand side plot all measurements have been corrected with the breathing model values. The break at $x \sim 7020$ shows the time of the mirror move of July 2009. Blue circles show focus measurements at any given science instrument (SI), while magenta diamonds show WFC3 UVIS channel results.

the WFC3 UVIS channel is below the nominal focus frame of ACS. Based on 17 measurements the mean difference between the two instruments is $\sim 0.54 \pm 0.20 \mu\text{m}$ (in the units of the secondary mirror displacement), where the error is the standard error of the mean.

Figure 6 also implies that the focus difference may be decreasing. Physically this may be possible due to outgassing of the WFC3. The outgassing could potentially, as in the case of the overall HST focus trend, cause the focus difference between the WFC3 UVIS channel and the ACS WFC to decrease exponentially before settling to a fixed value. This value may very well be smaller than the focus difference ($0.5 \mu\text{m}$) quoted above if outgassing takes a longer time than the baseline sampled. However, due to the large scatter in the data and the relatively small number of data points, it is difficult to draw any robust conclusions at this point. More measurements and a longer baseline are required for robust conclusions. Even so, we adopt $0.5 \mu\text{m}$ as the focus difference between the WFC3 UVIS and the ACS WFC in the following discussion.

4.4 Zero-focus Predictions

Using the fits and trends discussed in Sections 4.1 and 4.2, it is possible to predict a zero-focus crossing date for a given instrument. The zero-focus crossing marks the time when the telescope, on average, is on its best focus defined in the focus frame of ACS. The other science instruments have been set to be confocal to ACS (Lallo et al. 2010) (note however the discussion in the previous section). There is no need for an immediate action, i.e., refocusing,

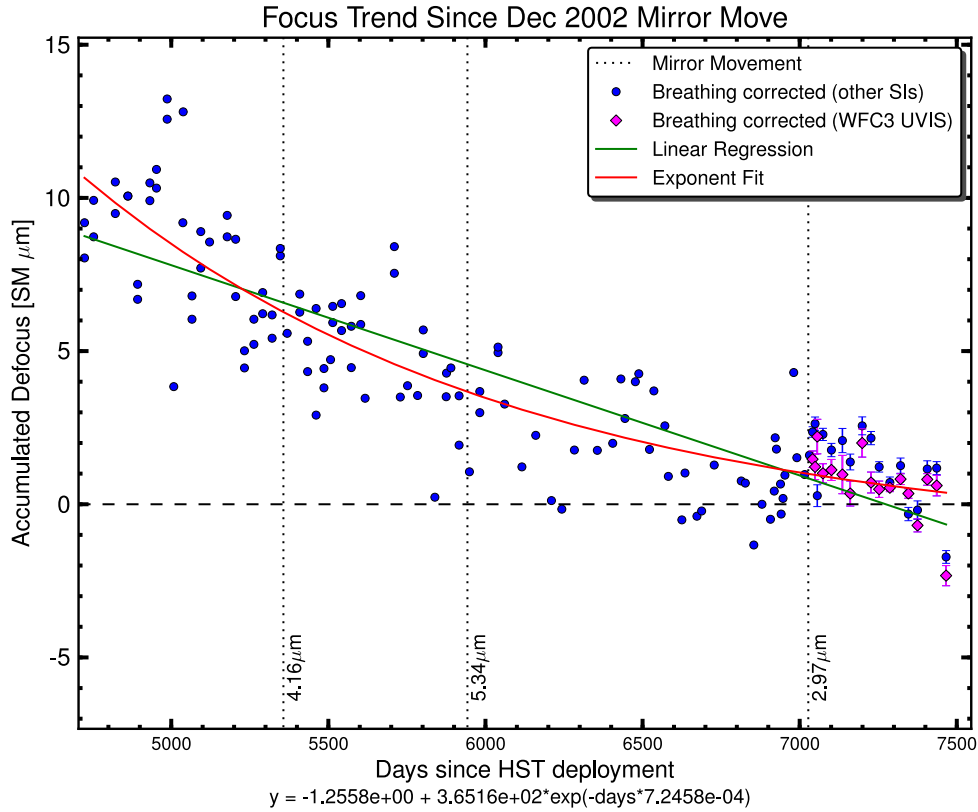


Figure 5. Focus measurements since the mirror move of December 2002. The latest mirror move (July 2009) has been taken into account. All values presented are corrected with the breathing model applied. The exponential fit is given below the x-axis label.

after the optimal (zero) focus has been passed. However, when the telescope is significantly¹ on the negative side (i.e. the secondary is too close to the primary mirror), a refocussing process is usually appropriate to bring the telescope and all the science instruments back in focus.

The zero-focus crossing predictions for ACS and for all instruments confocal to ACS are listed in Table 2. These predictions are based on different amounts of data and on different fitting functions, so the true zero-focus crossing date is most likely between the two extremes. The table indicates what data have been used for a given prediction, what type of a function was fitted and whether the data were corrected with the breathing model (BC). The offset in the last prediction corresponds to a situation where the $0.5 \mu\text{m}$ difference between WFC3 UVIS channel and ACS WFC has been taken into account by adding $0.5 \mu\text{m}$ to all WFC3 measurements. Table 3 lists the zero-focus crossing dates for the WFC3 UVIS channel. In these predictions we have assumed that the focus of the UVIS channel is $0.5 \mu\text{m}$ below the default ACS focus frame.

The zero-focus crossing predictions for the telescope and for all instruments confocal to

¹The threshold will be based on Cycle 17 and 18 experience with WFC3 and other science instruments.

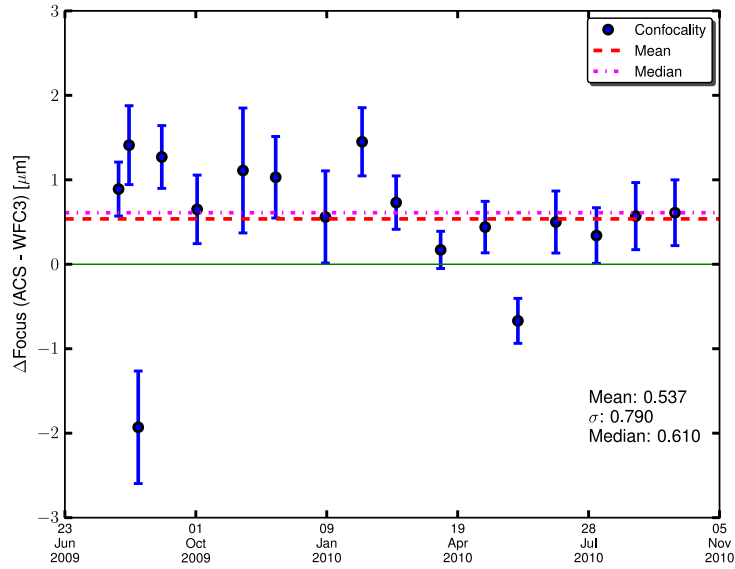


Figure 6. The focus difference between the ACS WFC and WFC3 UVIS channel. The errorbars shown have been obtained by adding the ACS and WFC3 errors in quadrature. The average focus difference is $\sim 0.5 \pm 0.2 \mu\text{m}$. Note, however, that the standard error of the mean is likely to be optimistic given the unexplained outliers and the existence of a possible trend.

ACS range from July 2010 to June 2012. In general, the historical trend has been found to provide a robust prediction. In this case the zero-focus crossing would take place in late November 2010. This prediction is in good agreement with a single exponential fit prediction when an offset of $0.5 \mu\text{m}$ to the WFC3 UVIS data has been applied, which predicts that the zero-focus crossing would take place in early December 2010. So at the time of this document was written, ACS (and all science instruments confocal to it) appear to be very close to its best focus.

Table 2. Predicted ACS zero-focus crossing dates based on historical data.

Data Used	Method	BC	Predicted Zero-focus Crossing
Since Launch	Double exponent	No	Monday 22, November, 2010
Since Dec 2002	Single exponent	No	Saturday 17, July, 2010
Since Dec 2002	Single exponent	Yes	Friday 01, June, 2012
Since Dec 2002	Single exponent + offset	No	Wednesday 01, December, 2010

Note: “BC” indicates Breathing Correction. If “Yes” then the focus values have been corrected with the breathing model values prior to fitting.

If the assumption that the WFC3 UVIS channel is $0.5\mu\text{m}$ below the ACS focus holds,

then the zero-focus crossing predictions are different (earlier) for the WFC3 UVIS channel (see Table 3). In this case the double exponential fit “predicts” that the WFC3 UVIS channel passed the optimal focus in March 2010, while the breathing corrected single exponential fit implies that the passing took place in October 2010. Note, however, that the assumption of $0.5\mu\text{m}$ focus difference between WFC3 and ACS is not robust, and hence these “predictions” should be interpreted with caution.

Table 3. Predicted WFC3 UVIS channel zero-focus crossing dates based on historical data when assuming that the UVIS channel is $0.5\mu\text{m}$ below the ACS focus frame.

Data Used	Method	BC	Predicted Zero-focus Crossing
Since Launch	Double exponent	No	Thursday 04, March, 2010
Since Dec 2002	Single exponent	No	Sunday 11, October, 2009
Since Dec 2002	Single exponent	Yes	Saturday 23, October, 2010

Note: “BC” indicates Breathing Correction. If “Yes” then the focus values have been corrected with the breathing model values prior to fitting.

5 Summary and Conclusions

We have described how the monthly focus monitoring of the HST is performed by using a Phase Retrieval technique. The Phase Retrieval consists of finding the phase that for a measured amplitude satisfies a given set of constraints. For the focus monitoring purposes Phase Retrieval can be taken as a process of trying to recover the wavefront error given a measurement of the Point Spread Function (PSF). The Zernike polynomials are a set of orthogonal polynomials that arise in the expansion of a wavefront function for optical systems with circular pupils. Hence, they are related to the classical aberrations and thus provide a convenient mathematical expression of the aberration content in a wavefront.

Results from the focus monitoring program, since the mirror move of July 2009, were presented. These results clearly show that the mirror move was successfully executed. The results also show that the WFC3 Phase Retrieval is mature enough to produce robust results. Moreover, the WFC3 UVIS channel focus measurements show overall smaller scatter than ACS WFC results. Hence, the WFC3 UVIS channel provides a robust data for HST focus monitoring purposes.

The historical trend since the deployment of the observatory continues to follow the double exponential decay. If the double exponential trend holds, the current focus changes can be assumed to be slow and small. In general, the zero-focus crossing is predicted to take place between July 2010 and June 2012, depending on the fit. The spread in the predictions arises from the uncertainties in our understanding in the long-term trend. Either way, ACS (and all science instruments confocal to it) are close to best focus at the time this document was written.

The confocality of ACS WFC and WFC3 UVIS channel was also discussed. The results imply that the WFC3 UVIS channel is $\sim 0.5 \pm 0.2 \mu\text{m}$ (in the units of the secondary mirror movement) below the ACS focus. However, the results also imply that the difference may be declining in time. Unfortunately, due to the relatively small number of data points and to the short baseline, it is complicated to assess whether this decline is significant or not and what the rate may be. More data and a longer baseline are required for more robust assessment.

Acknowledgments

SMN would like to thank Colin Cox for the help when trying to understand the HST breathing model and George Hartig for his patience when trying to explain WFC3 and ACS optics.

Bibliography

- Carter, R.: 1985, *Space Telescope Systems Description Handbook ST/SE-02*
- Di Nino, D., Makidon, R. B., Lallo, M., Sahu, K., Sirianni, M., and Casertano, S.: 2008, *Instrument Science Report ACS 03*
- Fienup, J. R., Marron, J. C., Schulz, T. J., and Seldin, J. H.: 1993, *Appl. Opt.* **32(10)**, 1747
- Hu, P. H., Stone, J., and Stanley, T.: 1989, *Journal of the Optical Society of America A* **6**, 1595
- Krist, J. E. and Burrows, C. J.: 1995, *Appl. Opt.* **34(22)**, 4951
- Krist, J. E. and Burrows, C. J.: 1997, *STScI Phase Retrieval Software (FITPSF) User's Guide*
- Lallo, M., Makidon, R. B., Casertano, S., Gilliland, R., and Stys, J.: 2005, *Instrument Science Report TEL 03*
- Lallo, M., van der Marel, R., Hartig, G., Cox, C., and Niemi, S.-M.: 2010, *Instrument Science Report TEL 02*
- Molodij, G. and Rousset, G.: 1997, *Journal of the Optical Society of America A* **14**, 1949
- Niemi, S.-M., Lallo, M., Hartig, G., and Cox, C.: 2010, *Instrument Science Report TEL 01*
- Wang, J. Y. and Silva, D. E.: 1980, *Appl. Opt.* **19(9)**, 1510

1 Appendix

1.1 Data

Table 4: HST focus monitoring data since SMOV 4.

Visit	Dataset	Date
02	IBCY02BLQ	2009-08-03
02	IBCY02BNQ	2009-08-03
02	JBCY02011	2009-08-03
03	IBCY03J8Q	2009-08-11
03	IBCY03JAQ	2009-08-11
03	JBCY03011	2009-08-11
04	IBCY04M4Q	2009-08-18
04	IBCY04M6Q	2009-08-18
04	JBCY04011	2009-08-18
05	IBCY05B7Q	2009-09-05
05	IBCY05B9Q	2009-09-05
05	JBCY05011	2009-09-05
06	IBCY06MEQ	2009-10-02
06	IBCY06MGQ	2009-10-02
06	JBCY06011	2009-10-02
07	IBCY07ERQ	2009-11-06
07	IBCY07ETQ	2009-11-06
07	JBCY07011	2009-11-06
08	IBCY08F2Q	2009-12-01
08	IBCY08F4Q	2009-12-01
08	JBCY08011	2009-12-01
09	IBCY09UQQ	2010-01-08
09	IBCY09USQ	2010-01-08
09	JBCY09011	2010-01-08
10	IBCY10BKQ	2010-02-05
10	IBCY10BMQ	2010-02-05
10	JBCY10011	2010-02-05
11	IBCY11UPQ	2010-03-03
11	IBCY11URQ	2010-03-03
11	JBCY11011	2010-03-03
12	IBCY12FTQ	2010-04-06
12	IBCY12FVQ	2010-04-06
12	IBCY12FXQ	2010-04-06
12	IBCY12FZQ	2010-04-06
12	IBCY12G1Q	2010-04-06
12	IBCY12G3Q	2010-04-06
12	IBCY12G5Q	2010-04-06
12	IBCY12G7Q	2010-04-06
12	JBCY12FUQ	2010-04-06
12	JBCY12FYQ	2010-04-06
12	JBCY12G2Q	2010-04-06
12	JBCY12G6Q	2010-04-06
37	IBCY37EXQ	2010-05-10
37	IBCY37EZQ	2010-05-10
37	IBCY37F1Q	2010-05-10
37	IBCY37F3Q	2010-05-10
37	IBCY37F5Q	2010-05-10
37	IBCY37F7Q	2010-05-10
37	IBCY37F9Q	2010-05-10
37	IBCY37FBQ	2010-05-10
37	JBCY37EYQ	2010-05-10
37	JBCY37F2Q	2010-05-10
37	JBCY37F6Q	2010-05-10
37	JBCY37FAQ	2010-05-10
38	IBCY38VLQ	2010-05-10
38	IBCY38VNQ	2010-05-10

Continued on next page

Table 4 – continued from previous page

Visit	Dataset	Date
38	IBCY38VPQ	2010-05-10
38	IBCY38VRQ	2010-05-10
38	IBCY38VTQ	2010-05-10
38	IBCY38VVQ	2010-05-10
38	IBCY38VXQ	2010-05-10
38	IBCY38VZQ	2010-05-10
38	JBCY38VMQ	2010-05-10
38	JBCY38VQQ	2010-05-10
38	JBCY38VUQ	2010-05-10
38	JBCY38VYQ	2010-05-10
39	IBCY39PNQ	2010-07-03
39	IBCY39PPQ	2010-07-03
39	IBCY39PRQ	2010-07-03
39	IBCY39PTQ	2010-07-03
39	IBCY39PVQ	2010-07-03
39	IBCY39PXQ	2010-07-03
39	IBCY39PZQ	2010-07-03
39	IBCY39Q1Q	2010-07-03
39	JBCY39POQ	2010-07-03
39	JBCY39PSQ	2010-07-03
39	JBCY39PWQ	2010-07-03
39	JBCY39Q0Q	2010-07-03
40	JBCY40IGQ	2010-08-03
40	JBCY40IKQ	2010-08-03
40	JBCY40IOQ	2010-08-03
40	JBCY40ISQ	2010-08-03
40	IBCY40IFQ	2010-08-03
40	IBCY40IHQ	2010-08-03
40	IBCY40IJQ	2010-08-03
40	IBCY40ILQ	2010-08-03
40	IBCY40INQ	2010-08-03
40	IBCY40IPQ	2010-08-03
40	IBCY40IRQ	2010-08-03
40	IBCY40ITQ	2010-08-03
17	JBCY17011	2010-09-02
17	IBCY17YGQ	2010-09-02
17	IBCY17YIQ	2010-09-02